APL Materials

Apparent auxetic to non-auxetic crossover driven by Co^{2+} redistribution in $CoFe_2O_4$ thin films

Cite as: APL Mater. **7**, 031109 (2019); https://doi.org/10.1063/1.5087559
Submitted: 02 January 2019 . Accepted: 08 March 2019 . Published Online: 25 March 2019

Elias Ferreiro-Vila, Lucia Iglesias, Irene Lucas del Pozo, Noa Varela-Dominguez, Cong Tinh Bui, Beatriz Rivas-Murias, Jose M. Vila-Fungueiriño, Pilar Jimenez-Cavero, Cesar Magen, Luis Morellon, Victor Pardo, and Francisco Rivadulla

Apparent auxetic to non-auxetic crossover driven by Co^{2+} redistribution in $CoFe_2O_4$ thin films

Cite as: APL Mater. 7, 031109 (2019); doi: 10.1063/1.5087559
Submitted: 2 January 2019 • Accepted: 8 March 2019 •
Published Online: 25 March 2019

Elias Ferreiro-Vila,[1] Lucia Iglesias,[1] Irene Lucas del Pozo,[2,3] Noa Varela-Dominguez,[1] Cong Tinh Bui,[1] Beatriz Rivas-Murias,[1] Jose M. Vila-Fungueiriño,[4] Pilar Jimenez-Cavero,[2,3] Cesar Magen,[3] Luis Morellon,[2,3] Victor Pardo,[5,6] and Francisco Rivadulla[1,a)]

AFFILIATIONS

[1]Centro de Investigación en Química Biolóxica e Materiais Moleculares (CIQUS), Universidade de Santiago de Compostela, 15782 Santiago de Compostela, Spain
[2]Instituto de Nanociencia de Aragón (INA), Departamento Física de la Materia Condensada, Universidad de Zaragoza, 50018 Zaragoza, Spain
[3]Instituto de Ciencia de Materiales de Aragón (ICMA), Universidad de Zaragoza-CSIC, Zaragoza, Spain and Departamento de Física de la Materia Condensada, Universidad de Zaragoza, 50009 Zaragoza, Spain
[4]Institut d'Électronique et des Systèmes (IES), UMR 5214, CNRS—Université de Montpellier, 860 Rue Saint Priest, 34095 Montpellier, France
[5]Departamento de Física Aplicada, Facultade de Física, Universidade de Santiago de Compostela, 15782 Santiago de Compostela, Spain
[6]Instituto de Investigacións Tecnolóxicas, Universidade de Santiago de Compostela, 15782 Santiago de Compostela, Spain

[a)]**Author to whom correspondence should be addressed:** f.rivadulla@usc.es

ABSTRACT

Oxide spinels of general formula AB_2O_4 (A = Mg^{2+}, Fe^{2+}; B = Al^{3+}, Cr^{3+}, etc.) constitute one of the most abundant crystalline structures in mineralogy. In this structure, cations distribute among octahedral and tetrahedral sites, according to their size and the crystal-field stabilization energy. The cationic arrangement determines the mechanical, magnetic, and transport properties of the spinel and can be influenced by external parameters like temperature, pressure, or epitaxial stress in the case of thin films. Here, we report a progressive change in the sign of the Poisson ratio, ν, in thin films of $CoFe_2O_4$, defining a smooth crossover from auxetic ($\nu < 0$) to non-auxetic ($\nu > 0$) behavior in response to epitaxial stress and temperature. Microstructural and magnetization studies, as well as *ab initio* calculations, demonstrate that such unusual elastic response is actually due to a progressive redistribution of Co^{2+} among the octahedral and tetrahedral sites of the spinel structure. The results presented in this work clarify a long standing controversy about the magnetic and elastic properties of Co-ferrites and are of general applicability for understanding the stress-relaxation mechanism in complex crystalline structures.

Oxygen ions in AB_2O_4 spinels arrange in a cubic close-packed (f.c.c.) lattice, with the A and B cations occupying 1/8 of the tetrahedral and 1/2 of the octahedral holes of the lattice.[1] On the basis of this distribution, spinels may be broadly classified in normal spinels, like $CoAl_2O_4$ or Mn_3O_4, in which the 2+ cations occupy the tetrahedral (Th) sites, and inverse spinels, like $MgFe_2O_4$ or Fe_3O_4, in which Mg^{2+} and Fe^{2+} respectively, occupy the octahedral (Oh) sites. The actual degree of inversion can be varied through pressure, temperature, or a combination of both. In the case of thin films, epitaxial stress is also expected to play a major role in the actual cationic distribution.[2]

An interesting case of study is that of $CoFe_2O_4$ (CFO), an insulating spinel in which Co^{2+} occupies the Oh-sites (inverse spinel), resulting in a large magnetic anisotropy.[3] This, combined with a high Curie temperature, makes CFO thin films very appealing for the fabrication of spin-filter tunnel barriers.[4–6] However, the elastic

response of this material to epitaxial stress is quite unique: Valant *et al.*[7] reported a negative Poisson ratio (auxetic behavior) in $CoFe_2O_4$ thin films deposited on $SrTiO_3$. This effect is extremely rare in crystalline materials and was tentatively attributed to a deformation of the hinge-like metal-oxygen bond network characteristic of the spinel structure. However, Foerster *et al.*[8] challenged these results and reported a non-auxetic behavior of $CoFe_2O_4$ on $SrTiO_3$ and $MgAl_2O_4$, but with an anomalously low Poisson ratio, highly dependent on the actual degree of stress. Although macroscopic and composite materials with complex internal structure showing auxetic behavior are known for long, molecular auxetic materials are very scarce.[9–11]

In this paper, we demonstrate that $CoFe_2O_4$ accommodates the epitaxial stress by a continuous migration of Co^{2+} from the Oh to Th sites, which results in dramatic changes in the magnetic anisotropy, and an apparent transition from molecular auxetic to non-auxetic behavior. We compare the results of a series of films synthesized by a chemical solution method (polymer assisted deposition, PAD;[12,13] see the supplementary material) and pulsed laser deposition (PLD), which allowed us to explore an unusually large range of epitaxial stress. Our results have important implications for the design of spin-filter barriers based on CFO for applications in spintronics, as well as for the understanding of structural relaxation in this important class of minerals, and in complex oxides in general.

The results of the structural analysis of the films are summarized in Fig. 1 ($\theta/2\theta$ X-ray diffraction) and in Figs. S1 and S2 (high-resolution X-ray reciprocal space maps, RSM) in the supplementary material. They correspond to a series of samples of $CoFe_2O_4$ deposited by PLD and PAD on (001) $MgAl_2O_4$ substrates, at different temperatures. $MgAl_2O_4$ (a = 8.09 Å) imposes a maximum in-plane compressive strain on CFO (a_b = 8.355 Å) of ≈3.3%. X-ray RSM show that the in-plane lattice parameter is slightly lower in the PLD than in the PAD films [Fig. 1(c)] indicating a better matching to the substrate. However, it is also evident that there is an additional contribution at lower Q_x (larger in-plane lattice parameter; see Figs. S1 and S2), showing the presence of a partially relaxed portion of the film. This was further corroborated by the analysis of high-angle annular dark-field (HAADF)-scanning transmission electron microscopy (STEM) data (see below). Consistent with an average larger in-plane compression, the *c*-axis elongation is also larger in PLD films with respect to PAD [Fig. 1(d)], as expected from an elastic deformation of the crystalline unit cell. Importantly, even when the average in-plane lattice parameter *a* obtained from X-ray diffraction is only slightly affected by a change in the deposition temperature, the *c*-axis length decreases continuously, being this tendency independent of the method of synthesis.

The continuous reduction of the *c*-axis length is completely unexpected *a priori*, given the small variations observed in the in-plane lattice parameter. Therefore, the observed decrease in *c* with temperature must reflect the accommodation of epitaxial compressive stress by some internal (molecular) degree of freedom of the spinel lattice.

The Poisson coefficient, ν, is the parameter that quantifies the relative changes of volume and shape of a system in response to an arbitrary mechanical stress:[14,15] $\nu = -\epsilon_t/\epsilon_l$; ϵ_t and ϵ_l represent the strain in the transverse and longitudinal directions to the uniaxial longitudinal stress, respectively. In response to a compressive (tensile) stress, most materials expand (contract) in the perpendicular direction. This behavior is reflected in a positive ν. On the other hand, materials with the negative Poisson ratio (auxetic or anti-rubber) expand in the perpendicular direction to the longitudinal tension.

For epitaxial thin films with biaxial (symmetric) in-plane stress, an effective Poisson ratio $\nu*$ can be defined[15]

$$\nu* = \frac{2\nu}{1-\nu}, \tag{1}$$

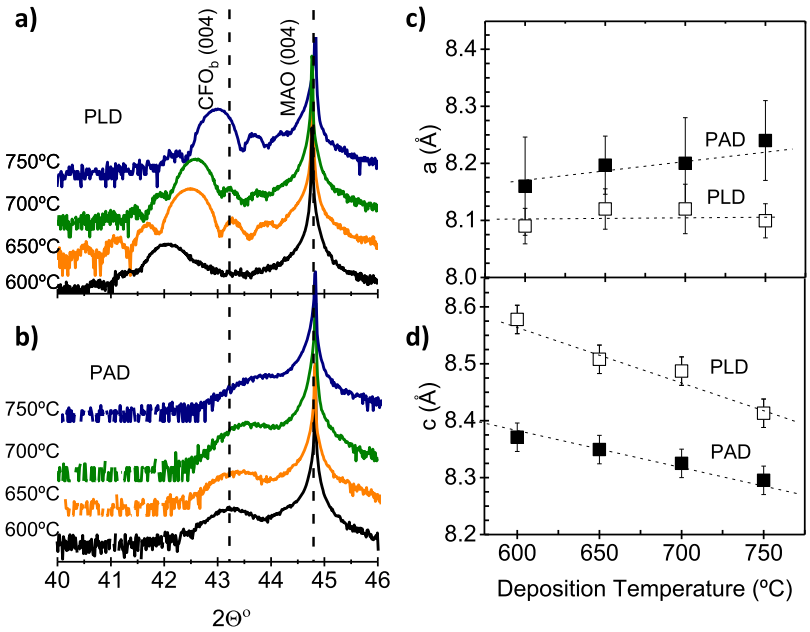

FIG. 1. $\theta/2\theta$ X-ray diffraction around the (004) Bragg reflection of the films deposited by PLD (a) and PAD (b), at different temperatures. The vertical dashed lines show the cubic lattice parameter of the inverse spinel CFO and the substrate. The variation of the *a* and *c* lattice parameters with the deposition temperature is shown in (c) and (d), respectively. These were derived from (a) and (b) and the X-ray reciprocal space maps shown in the supplementary material accompanying this paper (Figs. S1 and S2).

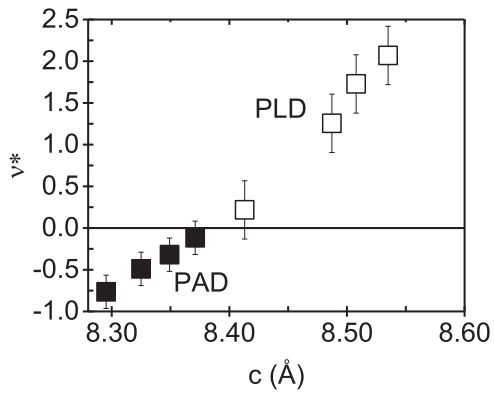

FIG. 2. Evolution of the Poisson ratio, ν^*, with the *c*-axis lattice parameter of the $CoFe_2O_4$ films. Open/closed symbols refer to films deposited by PLD/PAD, respectively. Negative (positive) ν^* indicates auxetic (non-auxetic) behavior (see text).

with $\epsilon_t = (c_f - c_b)/c_b$ and $\epsilon_l = (a_f - a_b)/a_b$; the subscripts f and b refer to the film and bulk, respectively. Expressing $\nu*$ as a function of the different elastic moduli defines its meaningful numerical limits, $-1 < \nu < 2$ in an isotropic material.[14,15] The evolution of $\nu*$ for the two sets of CFO films studied in this work is shown in Fig. 2.

A smooth crossover from negative to positive $\nu*$ as the *c* axis increases is clearly visible, defining a transition from auxetic to non-auxetic behavior in $CoFe_2O_4$. Samples synthesized by PLD show a non-auxetic behavior, although with a varying $\nu*$, whereas the films deposited by PAD, reveal an auxetic or anti-rubber behavior. It is the unique combination of deposition methods presented in this work what allows the exploration of an unusually wide range of lattice parameters, extending across the whole range of ν^*. Therefore, ν^* of $CoFe_2O_4$ thin films can be continuously tuned from ≈−1 to ≈+2. The values reported by Valant *et al.*[7] ($\nu^* < -0.85$) and Forerster *et al.*[8] ($\nu* \approx +0.27$-0.57) are within the range of values reported in this work.

Understanding the origin of this puzzling negative-to-positive crossover of $\nu*$ may give the key to understand the variation of physical properties reported in the literature from *a priori* similar films of CFO. As we will demonstrate, the most plausible source for this crossover is a continuous redistribution of Co^{2+} cations among the different sites of the spinel lattice, i.e., a change in the degree of inversion of the spinel, induced by epitaxial stress and temperature.

The atomic arrangement of the spinel lattice is shown in Fig. 3(a). The cations at the octahedral positions define a pyrochlore lattice of corner-sharing tetrahedra. This produces a trigonal crystal field at the octahedral sites, which breaks down the degeneracy of the T_{2g} manifold. When Co^{2+} occupies these positions (inverse spinel), the trigonal-field stabilizes a hole in the E_g doublet, therefore introducing a strong single-ion magnetocrystalline anisotropy via spin-orbit coupling [V_{LS}; Fig. 3(b)].[3] The anisotropy should decrease with temperature as the population of the E_g level increases, at a rate determined by the magnitude of V_t. Therefore, the magnetic anisotropy can be used as a sensitive probe to monitor the structural changes in response to epitaxial stress, either through a variation in the crystal-field energy (V_t splitting) or through a redistribution of Co^{2+} ions among the octahedral/tetrahedral sites.

Ab initio calculations show that the inverse spinel structure (Oh–Co^{2+}) is always the lowest energy solution for CFO. Figure 3(c) shows the energy of the normal spinel phase with respect to the ground state inverse spinel, as a function of the out of-plane lattice parameter for several values of the in-plane lattice parameter. Larger *a*-axes favor the progressive stabilization of the normal spinel (Th–Co^{2+}). Also, for a fixed value of *a*, increasing *c* favors the appearance of the normal spinel phase. Looking back at Fig. 1, the films grown by PAD, showing $\nu* < 0$, have a larger in-plane lattice parameter. According to our *ab initio* calculations in Fig. 3(c), this implies a

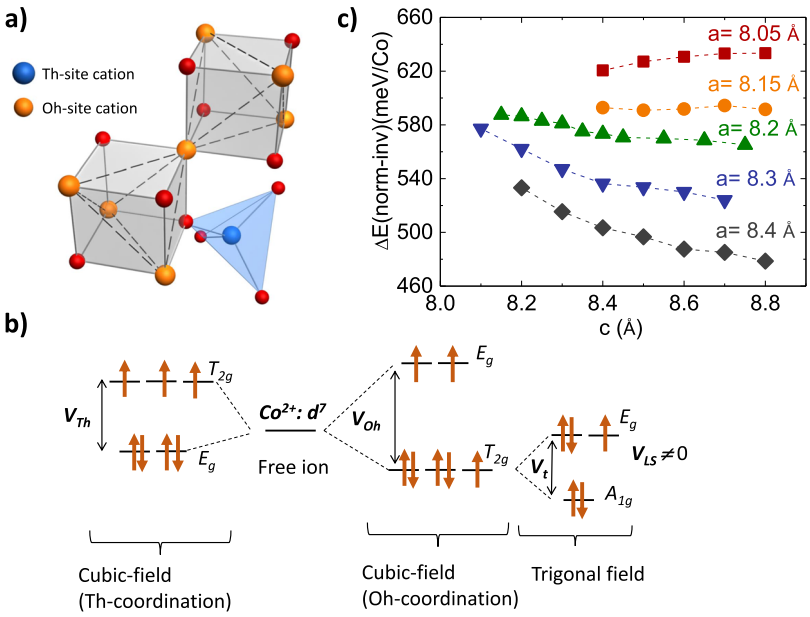

FIG. 3. (a) Detail of the crystalline structure of the spinel, showing the B-site coordination. Blue/orange cations occupy the tetrahedral/octahedral sites, respectively (oxygen ions in red). (b) Crystal-field splitting of the d^5 electron states (Mulliken notation) in an octahedral (right) or tetrahedral (left) environment. V_{Oh} and $V_{Th} \approx 0.44\ V_{Oh}$ refer to the octahedral and tetrahedral crystal field energy, respectively. Trigonal-field splitting of the cubic orbitals, with an energy $V_t \ll V_{Oh}$. (c) Calculated *ab initio* energy difference between the normal and the inverse spinel, as a function of the out of-plane lattice parameter, *c*, for different values of the in-plane lattice parameter, *a*. The inverse spinel is always the most stable phase from the *ab initio* calculations.

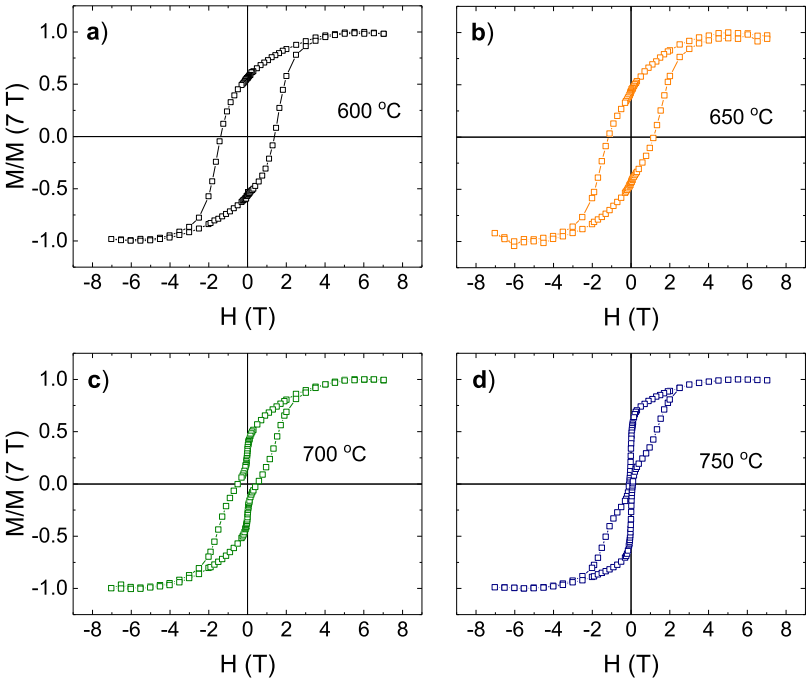

FIG. 4. [(a)–(d)] Magnetic hysteresis loops measured at 10 K for the films deposited by PAD at different temperatures.

smaller energy difference between the normal and the inverse spinel phases; thus, the degree of inversion will be smaller for the films grown in PAD than those grown by PLD.

The magnetization versus magnetic field M(H) hysteresis loops of the films deposited by PAD at different temperatures are shown in Fig. 4. Starting from a single hysteresis loop with $H_C \approx 1.7$ T for the samples deposited at the lower temperature (600°), there is a progressive contribution from a magnetically softer phase ($H_C \approx 0$ T), as the deposition temperature increases. PLD samples show similar behavior although the two-phase contribution is only observable at the highest deposition temperatures of 750 °C (Fig. S3 in the supplementary material).

The different contribution from the hard/soft magnetic phases can be better appreciated in the derivative of the M(H) curves, Fig. 5(a). Increasing the deposition temperature results in the growth of the peak at 0 T, while the position of the maximum close to 1.7 T does not change significantly with the deposition temperature but decreases its intensity. This suggests that the magnetically soft phase grows at the expense of the hard phase, as the deposition temperature increases.

On the other hand, the decrease in H_C with temperature reported in Fig. 5(b) provides valuable information about the distortion-induced trigonal crystal-field in the films. First, the larger values of H_C in the PLD films compared to PAD films suggest that the larger in-plane compression of the former produces a higher anisotropy (i.e., larger trigonal V_t splitting). Second, the rate of decrease dH_C/dT is similar for films deposited by the same method, i.e., with similar in-plane lattice parameter. This is in good agreement with the results from *ab initio* calculations: in-plane compression favors the inverse (hard magnetic) spinel phase.

All these results lead us to conclude that the combined effect of epitaxial strain and temperature produces a redistribution of Co^{2+} ions among the Oh and Th sites of the spinel. This is the origin of the two-phase behavior in the M(H) loops and of the apparent auxetic to non-auxetic transition reported in Fig. 2 of this paper. The continuous reduction in the *c*-axis of CFO reflects a continuous change

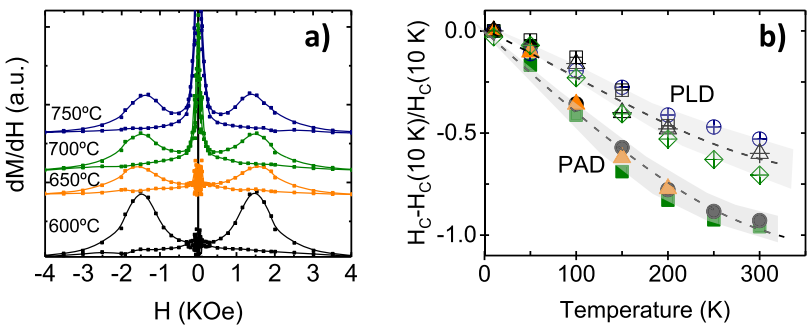

FIG. 5. (a) Magnetic field derivative of the M(H) curves shown in Fig. 4. The contribution from the soft phase, characterized by the height of the peak close to zero field, increases continuously with the deposition temperature. The curves have been displaced vertically for clarity. (b) Temperature dependence of H_C for the films deposited by PLD (open symbols) and PAD (closed symbols) at different temperatures.

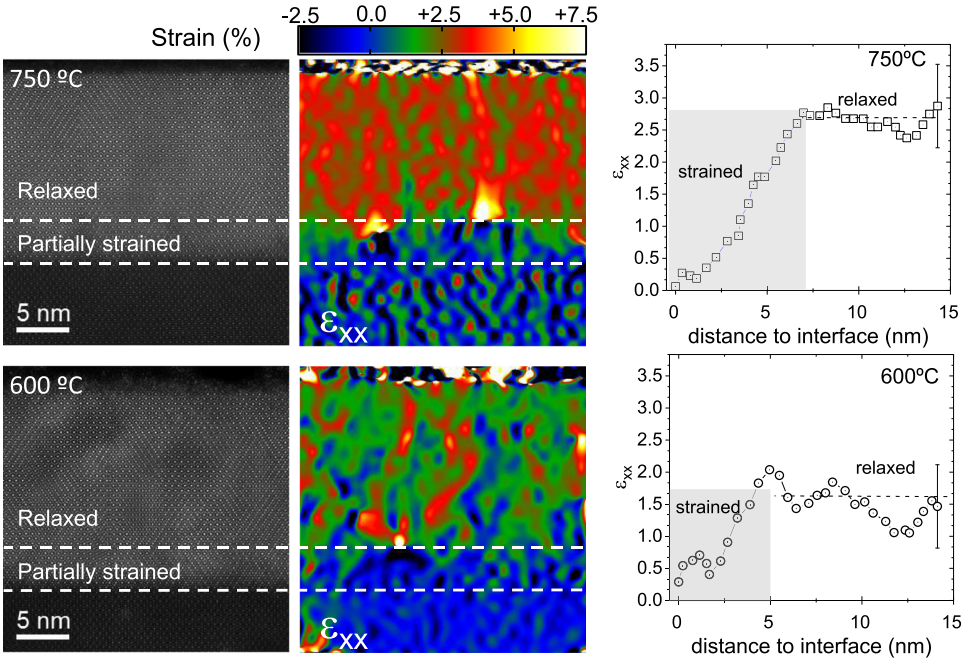

FIG. 6. HAADF-STEM image and GPA analysis of two films deposited by PLD at 600 °C (bottom) and 750 °C (top). GPA analysis and line-profile along the film thickness showing the in-plane elongation ε_{xx} with respect to the substrate, for the films deposited at 600 °C and 750 °C.

in the degree of inversion of the spinel. Therefore, the anomalous behavior of $v*$ reported in Fig. 2 and by other authors is an artifact by assuming, erroneously, the constant lattice parameters of bulk CFO in Eq. (1); instead, it is changing from point to point as the degree of inversion changes.

The origin of the two-loop M(H) curves in CFO was previously associated by Rigato *et al.*[16] to the presence of pyramid-like structures in the surface of CFO with a lower anisotropy than the bulk. The results presented in this work correspond to samples of the same thickness, synthesized by two different methods, which result in different morphologies and surface roughness. In Fig. S4, we show the X-ray reflectivity and AFM topography of the surface of two films deposited at 600 °C and 750 °C by PAD and PLD. Samples deposited by PAD show a more granular structure and surface roughness than films deposited by PLD. However, despite these large morphological differences, the magnetic behavior of the samples deposited at 750 °C is identical (see Fig. S3). We therefore rule out the possibility of a pure surface effect to explain these results observed in M(H). Other authors attributed the low-field contribution to M(H) to the nucleation of antiphase boundaries (APBs)[17,18] (see Fig. S5 in the supplementary material). APBs are defects which imply a half lattice displacement of the cations, reducing the crystalline order of the film and therefore their magnetization and coercivity. The concentration of these defects decreases as the mismatch with the substrate is reduced, and they are more prevalent at low thicknesses. Nevertheless, our PAD and PLD films are of the same thickness, and our careful microscopic study does not reveal a clear and systematic increase in APBs compatible with these observations (see also Fig. S6 in the supplementary material).

Therefore, the hypothesis of the increasing population of Th–Co^{2+} with temperature is the most plausible explanation of the magnetic and elastic behavior of CFO thin films.

In order to further characterize the extension of the soft/hard phases in the films, we performed high resolution scanning transmission electron microscopy (STEM) and geometrical phase analysis (GPA) of cross section lamellae. The results shown in Fig. 6 for two samples deposited by PLD at 600 °C and 750 °C (see also Fig. S3 for their magnetic behavior) corroborate the presence of a partially strained phase close to the interface with the substrate, which relaxes toward the surface of the film. The GPA analysis provides the evolution of the in-plane lattice parameter along the film thickness, while X-ray diffraction gives an average of the lattice parameter for the whole film. It is evident from our microscopic analysis that increasing the deposition temperature results in a larger portion of the film with a higher in-plane lattice parameter (relaxed). According to the previous discussion of the *ab initio* calculations, this will result in a larger contribution from the magnetically soft phase, in perfect agreement with the M(H) data shown in Fig. S3. A surface with softer magnetization than the bulk was deduced from magnetoresistance measurements.[19] Our results show that the thickness of this surface layer can be modulated by strain and temperature.

Finally, we want to mention that Sawatzky *et al.*[20] used Mössbauer spectroscopy to map the cationic distribution in $CoFe_2O_4$ ceramic powders undergoing different heat treatments. They found that increasing temperature results in a progressive reduction in the degree of inversion of the spinel, in agreement with our results.

In summary, the analysis of the structural and magnetic data of CFO thin films presented in this work demonstrate that this spinel accommodates the epitaxial stress by changing its degree of inversion. This is the origin of the two-phase M(H) loops and the anomalous v previously observed by other authors. Our results will help to understand the complex relaxation behavior observed in other multicationic oxides.[11]

Additional structural, microstructural, and magnetic details are provided in the supplementary material. Details of the calculations are also included.

This work has received financial support from Ministerio de Economía y Competitividad (Spain) under Project No. MAT2016-80762-R and MAT2017-82970-C2-R, Xunta de Galicia (Centro singular de investigación de Galicia accreditation 2016-2019, No. ED431G/09), the European Union (European Regional Development Fund-ERDF), and the European Commission through the Horizon H2020 funding by H2020-MSCA-RISE-2016-Project No. 734187–SPICOLOST. The microscopy studies have been conducted in the Laboratorio de Microscopías Avanzadas (LMA) at Instituto de Nanociencia de Aragón (INA)—Universidad de Zaragoza. Authors acknowledge the LMA-INA for offering access to their instruments and expertise. I.L.d.P. and B.R.-M. thank the funding under the ESTEEM2 project and the researchers L.A. Rodríguez and E. Snoeck for preliminary Lorentz Microscopy (L.M.) and electron holography (EH) studies in $CoFe_2O_4$ samples synthesized by PAD method performed at CEMES (Toulouse).

REFERENCES

[1] A. R. West, *Solid State Chemistry and its Applications* (John Wiley & Sons, 2014), ISBN: 978-1-119-94294-8.
[2] D. Fritsch and C. Ederer, Appl. Phys. Lett. **99**, 081916 (2011).
[3] J. B. Goodenough, *Magnetism and the Chemical Bond* (John Wiley & Sons, 1963).
[4] M. G. Chapline and S. X. Wang, Phys. Rev. B **74**, 014418 (2006).
[5] A. V. Ramos, T. S. Santos, G. X. Miao, M.-J. Guittet, J.-B. Moussy, and J. S. Moodera, Phys. Rev. B **78**, 180402 (2008).
[6] P. V. Lukashev, J. D. Burton, A. Smogunov, J. P. Velev, and E. Y. Tsymbal, Phys. Rev. B **88**, 134430 (2013).
[7] M. Valant, A. K. Axelsson, F. Aguesse, and N. M. Alford, Adv. Funct. Mater. **20**, 644 (2010).
[8] M. Foerster, M. Iliev, N. Dix, X. Martí, M. Barchuk, F. Sánchez, and J. Fontcuberta, Adv. Funct. Mater. **22**, 4344 (2012).
[9] K. E. Evans and A. Alderson, Adv. Mater. **12**, 617 (2000).
[10] C. Huang and L. Chen, Adv. Mater. **28**, 8079 (2016).
[11] S. Chen, C. Guan, S. Ke, X. Zeng, C. Huang, S. Hu, F. Yen, H. Huang, Y. Lu, and L. Chen, ACS Appl. Mater. Interfaces **10**, 18029 (2018).
[12] Q. X. Jia, T. M. McCleskey, A. K. Burrell, Y. Lin, G. E. Collis, H. Wang, A. D. Q. Li, and S. R. Foltyn, Nat. Mater. **3**, 529 (2004).
[13] J. M. Vila-Fungueirino, B. Rivas-Murias, J. Rubio-Zuazo, A. Carretero-Genevrier, M. Lazzari, and F. Rivadulla, J. Mater. Chem. C **6**, 3834 (2018).
[14] G. N. Greaves, A. L. Greer, R. S. Lakes, and T. Rouxel, Nat. Mater. **10**, 823 (2011).
[15] J. Y. Tsao, *Materials Fundamentals of Molecular Beam Epitaxy* (Academic Press, Inc., 1993), ISBN: 0-12-701625-2.
[16] F. Rigato, J. Geshev, V. Skumryev, and J. Fontcuberta, J. Appl. Phys. **106**, 113924 (2009).
[17] R. Datta, S. Kanuri, S. V. Karthik, D. Mazumdar, J. X. Ma, and A. Gupta, Appl. Phys. Lett. **97**, 071907 (2010).
[18] C. Gatel, B. Warot-Fonrose, S. Matzen, and J.-B. Moussy, Appl. Phys. Lett. **103**, 092405 (2013).
[19] M. Isasa, S. Vélez, E. Sagasta, A. Bedoya-Pinto, N. Dix, F. Sánchez, L. E. Hueso, J. Fontcuberta, and F. Casanova, Phys. Rev. Appl. **6**, 034007 (2016).
[20] G. A. Sawatzky, F. Van Der Woude, and A. H. Morrish, J. Appl. Phys. **39**, 1204 (1968).